INSTITUTE OF PHYSICS PUBLISHING NANOTECHNOLOGY
Nanotechnology **17** (2006) 3380–3387 doi:10.1088/0957-4484/17/14/007

Strain distributions in nano-onions with uniform and non-uniform compositions

H L Duan[1,2], B L Karihaloo[1,3], J Wang[2] and X Yi[2]

[1] School of Engineering, Cardiff University, Queen's Buildings, The Parade, Cardiff CF24 3AA, UK
[2] LTCS and College of Engineering, Peking University, Beijing 100871, People's Republic of China

E-mail: KarihalooB@Cardiff.ac.uk

Received 8 May 2006
Published 15 June 2006
Online at stacks.iop.org/Nano/17/3380

Abstract
Nano-onions are ellipsoidal or spherical particles consisting of a core surrounded by concentric shells of nanometre size. Nano-onions produced by self-assembly and colloidal techniques have different structures and compositions, and thus differ in the state of strains. The mismatch of the thermal expansion coefficients and lattice constants between neighbouring shells induces stress/strain fields in the core and shells, which in turn affect their physical/mechanical properties and/or the properties of the composites containing them. In this paper, the strains in embedded and free-standing nano-onions with uniform and non-uniform compositions are studied in detail. It is found that the strains in the nano-onions can be modified by adjusting their compositions and structures. The results are useful for the band structure engineering of semiconductor nano-onions.

(Some figures in this article are in colour only in the electronic version)

1. Introduction

The synthesis and characterization of particles with core–shell structures have attracted a lot of attention in many areas of science and technology. These particles, which are ellipsoidal or spherical in shape and which consist of a core surrounded by concentric shells of nanometre size, are called 'nano-onions' because of this special structure [1, 2]. In order to obtain target properties, different systems, in terms of materials and shell thickness (e.g. CdS/HgS/CdS, CdS/HgS/CdS/HgS/CdS), have been produced [3, 4]. Multi-fold core–shell structured particles of micrometre size are called 'micro-onions' [5]. Nano-onions can be used on their own as functional devices, besides being a constituent part of a composite medium [2, 6–10]. Nano-onions are a kind of quantum dot (QD). There are currently two leading methods for producing nanometre-size semiconductor quantum dots (QDs). The first is the self-assembled method [11, 12]. In this method, the quantum dot material is deposited on top of a substrate with a different lattice constant, and the resulting strain induces three-dimensional island growth (e.g. InAs/GaAs, InP/GaInP and $In_xGa_{1-x}As$/GaAs). The second method is colloidal, which can produce nearly spherical QDs (e.g. CdTe/CdSe and $CdTe_xSe_{1-x}$).

The alloyed QDs (e.g. $In_xGa_{1-x}As$, $CdTe_xSe_{1-x}$) have attracted much interest recently because the behaviour of any electronic devices made of these alloyed QDs is strongly affected by an enriched but non-uniform composition [13]. The possibility of tuning a particular composition profile via alloying is of great importance, as it represents another degree of freedom in the design of self-assembled hetero-epitaxial structures [14]. Hence, the assessment of composition profiles and strains is important to both the identification of the dominant growth mechanisms and the modelling of the confining potential of quantum dots [14, 15]. Many attempts have been made to measure the elastic strains and the compositions of QD structures by using different methods (e.g. atomic force microscopy, high-resolution electron microscope analysis, x-ray absorption, etc) [16–24]. For example, Rosenauer *et al* [18] evaluated the composition of $In_xGa_{1-x}As$/GaAs QD structure by measuring local lattice parameters and displacements, assuming a linear dependence of the lattice parameter on the In content (Vegard's law).

[3] Author to whom any correspondence should be addressed.

Quantitative analysis has been performed using transmission electron micrographs and finite-element modelling with the appropriate sample geometry [18]. Lelarge *et al* [20] obtained the strain distributions of $In_xGa_{1-x}As/InP$ QD structure by surface profile measurements using atomic force microscopy (AFM) and finite-element calculations. Bruls *et al* [23] performed cross-sectional scanning tunnelling microscopy and finite-element analysis of InAs QD with the shape of a truncated pyramid in a GaAs matrix and concluded that the dot consisted of InGaAs alloy with the In concentration increasing linearly towards the top of the dot. Rockenberger *et al* [24] studied a free-standing CdTe(core)/CdS(shell) nanoparticle by extended x-ray absorption. They observed changes in the bond lengths of CdTe and CdS, and concluded that small mismatches between the lattice parameters of the two materials can be elastically compensated by adjusting their lattice dimensions in a small interface layer, resulting in a strain. Therefore, they used the classical theory of elasticity to calculate the strain distribution within the core–shell structure by simulating the mismatch strain by a uniform prescribed eigenstrain in the core [24].

The mechanical behaviour of materials at the nanoscale is different from that at the macroscopic scale due to the increased ratio of the surface/interface to the volume. A classical continuum model to explain the surface effect on the elastic properties of nanostructures was formulated by Gurtin and Murdoch [25]. Later, it was further developed by many researchers [26–32] to analyse the elastic properties of nano-structured materials. Miller and Shenoy [26, 29] compared the results obtained by the classical continuum model with those obtained by the atomistic simulations for nanobeams and nanowires, and found that the two methods led to almost the same results. As a nanostructure can be regarded as a combination of a bulk and a surface [29], the mechanical behaviour of a nano-structured material can be predicted within the framework of continuum elasticity supplemented by surface elasticity [26, 29, 33]. In fact, Yakobson and Smalley [34] have noted that the laws of continuum mechanics are amazingly robust and allow one to treat even intrinsically discrete objects only a few atoms in diameter.

For heterogeneous electronic structures of fine scale, as pointed out by Itskevich *et al* [35], Little *et al* [36], and Pérez-Conde and Bhattacharjee [37], the misfit strain, the surface stress and the applied external pressure all modify the strain fields in them, and in turn affect the electronic structures, and hence their physical properties. Although the strain distributions of nano-structured materials (e.g. quantum dot structures) have been studied extensively using continuum approaches and atomistic simulations [38–46], no attempt has been made to calculate the strain distributions in nano-onions with non-uniform compositions, taking into account also the surface stress effect. Generally, the quantum dot and matrix are assumed to be isotropic in continuum approaches, and this assumption has been proved to be very reasonable when isotropic and anisotropic solutions for semiconductor materials were compared, and is thus widely used [38]. However, it should be noted that the sensitivity of some physical properties to strain could make anisotropic effects important and the isotropic approximation should therefore be treated with caution, particularly for layers oriented in certain crystallographic directions [39]. For most cases, however, the anisotropy only marginally modifies the strain distributions [39]. In this paper, we present a theoretical study of the strains in embedded and free-standing nano-onions of uniform and non-uniform compositions with surface/interface effect.

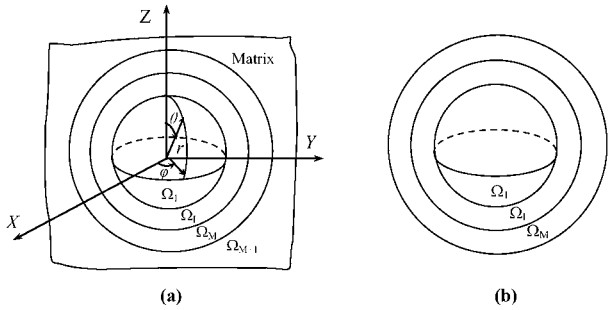

Figure 1. A spherical embedded nano-onion (a), and a spherical free-standing onion (e.g. CdS/HgS/CdS, ZnS/CdS/ZnS and CdS/HgS/CdS/HgS/CdS) (b).

2. Strain distributions in nano-onions with uniform composition

2.1. Embedded nano-onions

Consider a spherical nano-onion (a multi-shell spherical particle) embedded in an infinite elastic matrix, as shown in figure 1(a). Let phase 1 denote the innermost core, hereinafter referred to as the particle, and let phase I refer to the shell bounded by the concentric and spherical surfaces with radii r_I and $r_{I+1}(I \in (1, M))$, respectively. Let Ω_1, Ω_k $(k = 2, \ldots, I, \ldots, M)$ and Ω_{M+1} denote the regions occupied by the particle, the multi-shells and the matrix, respectively. The subscripts k $(k = 1, 2, \ldots I, \ldots, M, M+1)$ are used to denote the quantities in the regions Ω_k $(k = 1, 2, \ldots, I, \ldots, M, M+1)$, respectively. The interfaces between the particle and neighbouring shell and those between the shells further removed from the particle are perfectly bonded. The particle, the multi-shells and the matrix are homogeneous, linearly elastic and isotropic, characterized by the bulk modulus κ_k, the shear modulus μ_k and the Poisson's ratio ν_k $(k = 1, 2, \ldots, I, \ldots, M, M+1)$.

As in the work of Cahn and Larche [47], we choose the stress-free states of the spherical inclusion and its surrounding phases as their reference states. The strains induced by the mismatch of the lattice constants and thermal expansion coefficients in nano-onions can be treated as eigenstrains [24, 30, 40]. When uniform eigenstrains $\boldsymbol{\varepsilon}_I^*(I = 1, 2, \ldots, M)$ are prescribed in the particle and the multi-shells, the elastic strains $\boldsymbol{\varepsilon}^k(\mathbf{x})$ in the particle $(k = 1)$, the multi-shells $(k = 2, 3, \ldots, M)$, and the matrix $(k = M+1)$ can be expressed as

$$\boldsymbol{\varepsilon}^k = \mathbf{S}_I^k : \boldsymbol{\varepsilon}_I^* - \boldsymbol{\varepsilon}_k^* \qquad (k = 1, 2, \ldots, M+1). \tag{1}$$

It is noted that $\boldsymbol{\varepsilon}_{M+1}^* = \mathbf{0}$ in the above equation. $\mathbf{S}_I^k$ is the Eshelby tensor in the kth phase, which relates the uniform eigenstrain $\boldsymbol{\varepsilon}_I^*$ prescribed in the Ith phase to the strain induced

in the kth phase [48]. Thus the repeated subscript I in equation (1) indicates summation from 1 to M. As stated in section 1, the large ratio of surface/interface atoms to the bulk can have a profound effect on the properties of nanostructures, and this effect can be described by the classical continuum model with consideration of the interface effect. Therefore, the interface and boundary conditions to determine $\mathbf{S}_I^k$ are as follows [30]:

$$\begin{aligned} \mathbf{u}_I + \boldsymbol{\varepsilon}_I^* \cdot \mathbf{x} &= \mathbf{u}_{I+1} + \boldsymbol{\varepsilon}_{I+1}^* \cdot \mathbf{x}, \\ (\boldsymbol{\sigma}_I - \boldsymbol{\sigma}_{I+1}) \cdot \mathbf{N} &= \nabla_S \cdot \boldsymbol{\sigma}^s, \\ \mathbf{u}_{M+1} = \mathbf{0}, \qquad \boldsymbol{\sigma}_{M+1} &= \mathbf{0} \quad \text{at} \quad |\mathbf{x}| \to +\infty, \end{aligned} \tag{2}$$

where $\mathbf{x}$ is the position vector and $\mathbf{N}$ is the unit normal vector to the interface between the Ith and $(I+1)$ th phases, and $\nabla_S \cdot \boldsymbol{\sigma}^s$ denotes the interface divergence of the interface stress tensor $\boldsymbol{\sigma}^s$. Details are given in [30]. $\mathbf{S}_I^k$ satisfying the conditions equation (2) can be determined following the same procedure as used by Duan *et al* [49] in determining the Eshelby tensor in the absence of interface stress $\boldsymbol{\sigma}^s$.

The interface stress $\boldsymbol{\sigma}^s$ depends on the state of the elastic strain $\boldsymbol{\varepsilon}^s$ [27, 50, 51] and $\boldsymbol{\sigma}^s = \boldsymbol{\sigma}_0 + \mathbf{S} : \boldsymbol{\varepsilon}^s$ [26], where $\boldsymbol{\sigma}_0$ is the initial interface stress and $\mathbf{S}$ is the interface modulus tensor. However, the interface moduli are difficult to determine, and no data are currently available for the semiconductor materials. Therefore, without loss of the physical essence, in this paper we only consider a constant isotropic interface stress $\boldsymbol{\sigma}^s (= \sigma_0 \mathbf{1})$, where $\mathbf{1}$ is the second-order unit tensor in two-dimensional space.

2.2. Free-standing nano-onions

Figure 1(b) shows a spherical free-standing nano-onion consisting of a core and concentric multi-shells of nanometre size. Besides the uniform eigenstrains $\boldsymbol{\varepsilon}_I^*$ $(I = 1, 2, \ldots, M-1)$ prescribed in the particle and the multi-shells, we also assume that an isotropic surface stress vector $\boldsymbol{\tau}$ $(\boldsymbol{\tau} = \tau \mathbf{1}$; we distinguish it from the interface stress $\boldsymbol{\sigma}_0)$ and an external hydrostatic pressure P_{ex} act on the outer surface of the nano-onion. Then the elastic strains in the core and the multi-shells are

$$\boldsymbol{\varepsilon}^k = \mathbf{S}_I^k : \boldsymbol{\varepsilon}_I^* - \boldsymbol{\varepsilon}_k^* + \mathbf{E}^k(\boldsymbol{\tau}, P_{\text{ex}}) \qquad (k = 1, 2, \ldots, M). \tag{3}$$

Here the procedures used to obtain $\mathbf{S}_I^k$ are similar to those used to obtain the Eshelby tensors for the embedded nano-onion mentioned above. However, the interface and boundary conditions for this case are

$$\begin{aligned} \mathbf{u}_I + \boldsymbol{\varepsilon}_I^* \cdot \mathbf{x} &= \mathbf{u}_{I+1} + \boldsymbol{\varepsilon}_{I+1}^* \cdot \mathbf{x}, \\ (\boldsymbol{\sigma}_I - \boldsymbol{\sigma}_{I+1}) \cdot \mathbf{N} &= \nabla_S \cdot \boldsymbol{\sigma}^s, \\ \boldsymbol{\sigma}_{\text{M}} \cdot \mathbf{N} &= \mathbf{0} \qquad \text{at} \quad |\mathbf{r}| \to r_{\text{M}}. \end{aligned} \tag{4}$$

It is noted that $\boldsymbol{\varepsilon}_{\text{M}}^* = \mathbf{0}$ in the present case and $I \in (1, M-1)$ in equations (3) and (4). $\mathbf{E}^k(\tau, P_{\text{ex}})$ in equation (3) is the elastic strain tensor in the core and shells due to the surface stress τ and exterior hydrostatic pressure P_{ex}. The displacement fields in the core and shells due to τ and P_{ex} are

$$u_r^k(\tau, P_{\text{ex}}) = F_k r + \frac{G_k}{r^2} \qquad (k = 1, 2, \ldots, M), \tag{5}$$

and the components of $\mathbf{E}^k(\tau, P_{\text{ex}})$ in the spherical coordinates are

$$\begin{aligned} E_{rr}^k(\tau, P_{\text{ex}}) &= F_k - \frac{2G_k}{r^3}, \\ E_{\theta\theta}^k(\tau, P_{\text{ex}}) = E_{\varphi\varphi}^k(\tau, P_{\text{ex}}) &= F_k + \frac{G_k}{r^3}, \end{aligned} \tag{6}$$

where $G_1 = 0$ and the non-vanishing constants F_k and G_k are determined from the continuity conditions of the displacement and stress fields at the interfaces between the shells, and the following boundary conditions at the outermost boundary ($r = r_{\text{M}}$):

$$\sigma_{rr}^{\text{M}} = -\frac{2\tau}{r_{\text{M}}} - P_{\text{ex}}. \tag{7}$$

It is noted that equations (1) and (3) can apply to arbitrary uniform eigenstrains $\boldsymbol{\varepsilon}_I^*$ prescribed in the core and multi-shells.

For QD structures with a uniform composition, the mismatch of the lattice constants or thermal expansion coefficients of different constituents can induce an initial misfit strain. According to the definitions of an embedded QD [40] and a free-standing core–shell particle [24], the misfit strains arising from the different lattice constants and the thermal expansion coefficients between different phases are, respectively,

$$\varepsilon_{m0}^* = \frac{a_{\text{in}} - a_{\text{ex}}}{a_{\text{ex}}}, \qquad \varepsilon_{tm0}^* = (\alpha_{\text{in}} - \alpha_{\text{ex}})\Delta T, \tag{8}$$

where a_{in}, a_{ex} and α_{in}, α_{ex} are the lattice constants and the thermal expansion coefficients of the interior and exterior phases, respectively. ΔT is the temperature difference. For example, the misfit strain due to the mismatch of the lattice constants of the CdTe(core)/CdS(shell) structure is 11.6%, and that of ZnS(core)/CdS(shell) is −7.0%.

3. Strain distributions in nano-onions with non-uniform composition

The first expression in equation (8) is the so-called Vegard's law [52]. It is noted that Vegard's law for alloyed materials is a linear function: $E_{\text{alloy}} = xE_{\text{A}} + (1-x)E_{\text{B}}$, where E_{A}, E_{B} and E_{alloy} are the respective properties of pure A, pure B and the alloy A_xB_{1-x}, and x is the fraction of one ingredient in a material point [53]. For example, experiments have shown that the lattice constant of the non-uniform nano-onion ($Zn_xCd_{1-x}S$) exhibits a nearly linear relation with the Zn content x, which is consistent with Vegard's law [54, 55]. In the following, we assume that a spherical nano-onion has a spherically symmetric composition, i.e. the non-uniform composition is a function of the radial co-ordinate r only. Therefore, the misfit eigenstrain $\boldsymbol{\varepsilon}^*(r)$ induced by the mismatch of the lattice constants and the thermal expansion coefficients can be expressed as

$$\boldsymbol{\varepsilon}^*(r) = \varepsilon_m^*(r)(\mathbf{e}_r \otimes \mathbf{e}_r + \mathbf{e}_\theta \otimes \mathbf{e}_\theta + \mathbf{e}_\varphi \otimes \mathbf{e}_\varphi), \tag{9}$$

where $\mathbf{e}_r$, $\mathbf{e}_\theta$ and $\mathbf{e}_\varphi$ are the *local* unit base vectors in the spherical coordinate system, and $\varepsilon_m^*(r)$ is the misfit strain. The misfit strains induced by the lattice constants and thermal expansion coefficients are [46]

$$\varepsilon_m^*(r) = x(r)\varepsilon_{m0}^*, \qquad \varepsilon_m^*(r) = x(r)\varepsilon_{tm0}^*, \tag{10}$$

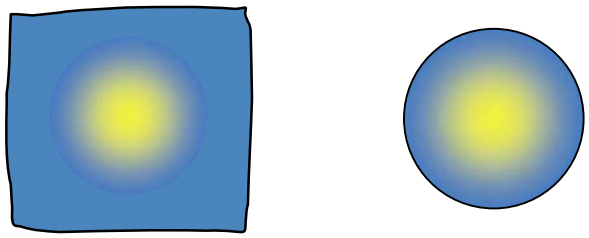

(a) (b)

Figure 2. A spherical embedded nano-onion with non-uniform composition (e.g. $In_xGa_{1-x}As$) (a), and a spherical free-standing nano-onion with a non-uniform composition (e.g. $CdTe_xSe_{1-x}$) in the core (b).

where x is the fraction of the ingredient at location r. If $x \equiv 1$, equation (10) reduces to those of a uniform composition (equation (8)).

The non-uniform distribution of the eigenstrain will result in an elastic field in a free-standing particle, namely the core of the nano-onion, even when the surface of the particle is not constrained. Therefore, in order to determine the elastic fields in an embedded nano-onion (figure 2(a)) and a free-standing core–shell nano-onion (figure 2(b)) induced by the non-uniform eigenstrain in equation (10), we first seek the elastic field in a free-standing core. According to the theory of elasticity, the governing equation for obtaining the eigen-displacement vector $\mathbf{u}^*$ is as follows:

$$C_{ijkl}(u^*_{k,lj} - \varepsilon^*_{kl,j}) = 0, \tag{11}$$

where the eigenstrain ε^*_{ij} is given in equation (9) and C_{ijkl} is the elastic moduli tensor of the core. Next, in order to obtain simple analytical solutions, we assume that the elastic moduli of the non-uniform core are constant, i.e. for example, the elastic moduli of the $In_xGa_{1-x}As$ core are those of InAs and the elastic moduli of the $CdTe_xSe_{1-x}$ core are those of CdTe. This is a reasonable assumption, because the compounds in the core have usually nearly identical elastic constants. Substituting equation (10) into (11), it follows that the only non-vanishing component of the displacement vector $\mathbf{u}^*$, viz $u^*_r(r)$ must satisfy the equation

$$r^2\frac{\partial^2 u^*_r}{\partial r^2} + 2r\frac{\partial u^*_r}{\partial r} - 2u^*_r - \frac{(1+\nu_1)}{(1-\nu_1)}\varepsilon^*_{m0}r^2\frac{\partial x}{\partial r} = 0, \tag{12}$$

where ν_1 is the Poisson ratio of the core. Therefore, equation (12) and the corresponding boundary conditions constitute the basic equations for finding $u^*_r(r)$. For a known variation of x, e.g. it could vary in a linear, logarithmic or exponential manner with r, $u^*_r(r)$ can be determined easily. In particular, if $x(r)$ in equation (10) is assumed to be a linear function in the radial co-ordinate r

$$x(r) = b_0 + b_1\frac{r}{r_{co}}, \tag{13}$$

where b_0 and b_1 are two constants and r_{co} denotes the radius of the non-uniform core, then the corresponding $u^*_r(r)$ is given by equation (12)

$$u^*_r(r) = rD_1 + \frac{D_2}{r^2} + \frac{b_1(1+\nu_1)r^2\varepsilon^*_{m0}}{4r_{co}(1-\nu_1)}. \tag{14}$$

The constants D_1 and D_2 are determined from the traction-free condition at the outer boundary of the free core and the condition for avoiding the singularity at the origin, and are

$$D_1 = b_0\varepsilon^*_{m0} + \frac{(1-2\nu_1)b_1\varepsilon^*_{m0}}{2(1-\nu_1)}, \qquad D_2 = 0. \tag{15}$$

It is seen that, even when the surface of the nano-particle is not constrained, the non-uniform eigenstrain still causes an elastic stress/strain field in the particle. When the non-uniform core is embedded in an infinite (relative to the core size) or finite alien medium, the constraint imposed by the exterior medium will cause an additional elastic field. In what follows, we will calculate this field by embedding the non-uniform core in an infinite medium or a finite shell. For the embedded nano-onion shown in figure 2(a), the displacement fields in the core and the matrix are given by equation (5) with $k = 1$ and $k = 2$, respectively, and $F_2 = 0, G_1 = 0$. The constants F_1 and G_2 are determined from the following interface conditions:

$$u^2_r = u^1_r + u^*_r\,|_{r=r_{co}}, \qquad \sigma^2_{rr} - \sigma^1_{rr} = \frac{2\sigma_0}{r_{co}}, \tag{16}$$

where u^1_r is the displacement in the core caused only by the constraint imposed by the matrix, and u^2_r is the total displacement in the matrix. For the embedded nano-onion with non-uniform composition, the components of the elastic strains $\boldsymbol{\varepsilon}^1$ and $\boldsymbol{\varepsilon}^2$ in the non-uniform core and the uniform matrix due to the above-mentioned linear radial misfit strain are, in spherical coordinates,

$$\begin{aligned}
\varepsilon^1_{rr} &= -\frac{\mu_2(H\varepsilon^*_{m0} + 2\sigma^*_0)}{3\kappa_1 + 4\mu_2} + \varepsilon^R_{rr},\\
\varepsilon^1_{\theta\theta} &= \varepsilon^1_{\varphi\varphi} = -\frac{\mu_2(H\varepsilon^*_{m0} + 2\sigma^*_0)}{3\kappa_1 + 4\mu_2} + \varepsilon^R_{\theta\theta},
\end{aligned} \tag{17}$$

$$\varepsilon^2_{rr} = -2\varepsilon^2_{\theta\theta} = -2\varepsilon^2_{\varphi\varphi} = -\frac{(3H\varepsilon^*_{m0}\kappa_1 - 8\mu_2\sigma^*_0)r^3_{co}}{2(3\kappa_1 + 4\mu_2)r^3}, \tag{18}$$

in which

$$\begin{aligned}
\varepsilon^R_{rr} &= \frac{\varepsilon^*_{m0}b_1}{2(1-\nu_1)}\left[1 - 2\nu_1 - (1-3\nu_1)\frac{r}{r_{co}}\right],\\
\varepsilon^R_{\theta\theta} &= \frac{\varepsilon^*_{m0}b_1}{4(1-\nu_1)}\left[2 - 4\nu_1 - (3-5\nu_1)\frac{r}{r_{co}}\right],
\end{aligned} \tag{19}$$

where $H = 4b_0 + 3b_1$, $\sigma^*_0 = \sigma_0/(r_{co}\mu_2)$, and κ_1, κ_2 and μ_1, μ_2 are the bulk moduli and shear moduli of the core and the infinite matrix, respectively.

The free-standing nano-onion is assumed to be composed of a non-uniform core and a uniform shell with the non-uniform eigenstrain $\boldsymbol{\varepsilon}^*$ prescribed in the core. Also, an isotropic surface stress τ and an external hydrostatic pressure P_{ex} are exerted at the outer surface of the shell. According to the superposition principle of the elasticity theory, the total elastic strains are equal to the sum of the strains caused by the three factors ($\boldsymbol{\varepsilon}^*$, τ and P_{ex}). The procedure for obtaining the solution due to $\boldsymbol{\varepsilon}^*$ is similar to that for the embedded onions. Therefore, the components of the elastic strain tensors $\boldsymbol{\varepsilon}^1$ and $\boldsymbol{\varepsilon}^2$ in the non-uniform core and the uniform shell are

$$\varepsilon^1_{rr} = -\frac{\Lambda_1}{3\chi} + \varepsilon^R_{rr}, \qquad \varepsilon^1_{\theta\theta} = \varepsilon^1_{\varphi\varphi} = -\frac{\Lambda_1}{3\chi} + \varepsilon^R_{\theta\theta}, \tag{20}$$

$$\varepsilon^2_{rr} = \Lambda_2 - \frac{2\Lambda_3 r^3_{co}}{r^3}, \qquad \varepsilon^2_{\theta\theta} = \varepsilon^2_{\varphi\varphi} = \Lambda_2 + \frac{\Lambda_3 r^3_{co}}{r^3}, \tag{21}$$

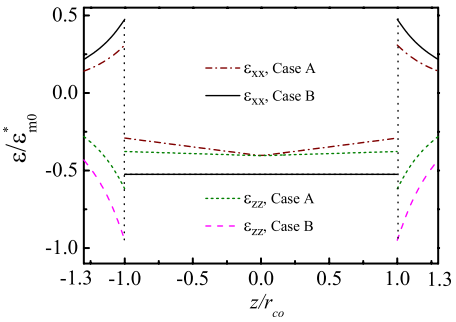

Figure 3. Distributions of normalized elastic strains $\varepsilon_{zz}/\varepsilon^*_{m0}$ and $\varepsilon_{xx}/\varepsilon^*_{m0}$ in the embedded nano-onion $In_xGa_{1-x}As/GaAs$ structure subjected to an eigenstrain $\boldsymbol{\varepsilon}^*$ in equation (9).

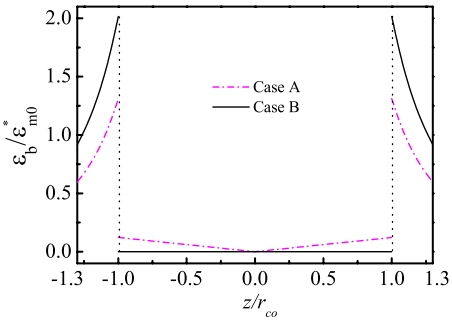

Figure 4. Distribution of normalized biaxial strain $\varepsilon_b/\varepsilon^*_{m0}$ in the embedded nano-onion $In_xGa_{1-x}As/GaAs$ structure subjected to an eigenstrain $\boldsymbol{\varepsilon}^*$ in equation (9).

with

$$\Lambda_1 = \mu_2[3(1-\rho_1^3)H\varepsilon^*_{m0}\kappa_2 + 2(3\kappa_2 + 4\rho_1^3\mu_2)\sigma_0^*] + (3\kappa_2 + 4\mu_2)(P_{ex} + 2\mu_2\tau^*),$$

$$\Lambda_2 = \frac{\rho_1^3\mu_2(3H\varepsilon^*_{m0}\kappa_1 - 8\mu_2\sigma_0^*)}{3\chi} - \frac{(3\kappa_1 + 4\mu_2)(P_{ex} + 2\mu_2\tau^*)}{3\chi}, \quad (22)$$

$$\Lambda_3 = \frac{\kappa_2(3H\varepsilon^*_{m0}\kappa_1 - 8\mu_2\sigma_0^*)}{4\chi} + \frac{(\kappa_1 - \kappa_2)(P_{ex} + 2\mu_2\tau^*)}{\chi},$$

$$\chi = 4(1-\rho_1^3)\kappa_2\mu_2 + \kappa_1(3\kappa_2 + 4\rho_1^3\mu_2),$$

where $\tau^* = \tau/(r_{sh}\mu_2)$, κ_1, κ_2 and μ_1, μ_2 are the bulk moduli and shear moduli of the core and shell, respectively. $\rho_1 = r_{co}/r_{sh}$, where r_{sh} denotes the outer radius of the shell.

4. Numerical results

For semiconductor structures, the important combinations of the strain components are the hydrostatic strain ε_h,

$$\varepsilon_h = \varepsilon_{xx} + \varepsilon_{yy} + \varepsilon_{zz}, \quad (23)$$

and the biaxial strain ε_b [45],

$$\varepsilon_b = \sqrt{(\varepsilon_{xx} - \varepsilon_{yy})^2 + (\varepsilon_{yy} - \varepsilon_{zz})^2 + (\varepsilon_{zz} - \varepsilon_{xx})^2}, \quad (24)$$

because ε_h usually shifts the conduction-band and valence-band edges and ε_b modifies the valence bands by splitting the degeneracy of light- and heavy-hole bands [39].

It is noted that the elastic moduli of nano-structured QDs are different from those of bulk materials due to the increased ratio of the surface to the volume. The elastic moduli of nanoparticles (or nanowires and nanofilms, etc) can be characterized by apparent (or effective) moduli, which reflect the surface effect [29, 33, 56, 57], and a simple scaling law for the properties of nano-structured materials has been given by Wang *et al* [33]. However, because of the lack of information on the surface properties of QDs under consideration, we cannot determine the exact effective elastic moduli of nano-structured QDs. Therefore, we make two approximations in the numerical calculations to follow. First, we neglect the effect of interface stress (i.e. $\boldsymbol{\sigma}_0$). However, as the effect of the surface stress (i.e. $\boldsymbol{\tau}$) on the outer surface of the shell can be very important for nanoparticles [58], we consider the effect of a surface stress in the free-standing nano-onion. Second, the elastic moduli of nano-structured QDs are assumed to be the same as those of the corresponding bulk materials.

4.1. Embedded nano-onion with non-uniform composition

In the following, we will analyse the elastic strain distribution in the embedded nano-onion $In_xGa_{1-x}As$ (core)/GaAs(matrix) (figure 2(a)) due to the misfit strain described by equations (10) and (13). It is noted that the embedded nano-onion InAs (figure 1(a), $M = 1$) is a special case of $In_xGa_{1-x}As$ (with $x(r) = 1$). The radius of the core $In_xGa_{1-x}As$ is $r_{co} = 9$ nm, and the lattice constants of InAs and GaAs are $a = 6.0584$ Å, $a = 5.6532$ Å, respectively. The elastic constants of bulk InAs and GaAs are as follows: InAs—bulk modulus 71.7 GPa, Poisson's ratio 0.267; GaAs—bulk modulus 92.8 GPa, Poisson's ratio 0.236 [59]. For the $In_xGa_{1-x}As$ core, we consider two radial compositional profiles of the core (equation (13): Case A—$b_0 = 0.8, b_1 = -0.2$; Case B—$b_0 = 1, b_1 = 0$. Case B corresponds to a core of uniform composition. Figure 3 shows the distributions of the normalized elastic strains $\varepsilon_{zz}/\varepsilon^*_{m0}$ and $\varepsilon_{xx}/\varepsilon^*_{m0}$ in the $In_xGa_{1-x}As/GaAs$ structure. The results show that the ratios of $\varepsilon_{zz}/\varepsilon^*_{m0}$ and $\varepsilon_{xx}/\varepsilon^*_{m0}$ in the $In_xGa_{1-x}As/GaAs$ structure are greatly affected by the composition. For the uniform core (InAs/GaAs) structure, the elastic strain in the core is also uniform, and the curves of ε_{xx} and ε_{zz} merge into one in the core, whereas the elastic strains in the non-uniform core of $In_xGa_{1-x}As/GaAs$ are non-uniform. Moreover, the InAs/GaAs system has a constant hydrostatic strain (ε_h) in the core and zero hydrostatic strain in the matrix (Case B), whereas for the $In_xGa_{1-x}As/GaAs$ system the hydrostatic strain is not uniform in the core (Case A). The variation in $\varepsilon_b/\varepsilon^*_{m0}$ is shown in figure 4. In the InAs/GaAs system, $\varepsilon_b = 0$ inside the core (Case B), whereas for the $In_xGa_{1-x}As/GaAs$ system, ε_b does not vanish (Case A). The biaxial strain in the matrix is positive and is a function of the position, decaying with the distance away from the core/matrix interface in both the InAs/GaAs and $In_xGa_{1-x}As/GaAs$ systems. Such a strain can modify the confining potential, leading to carrier localization [39].

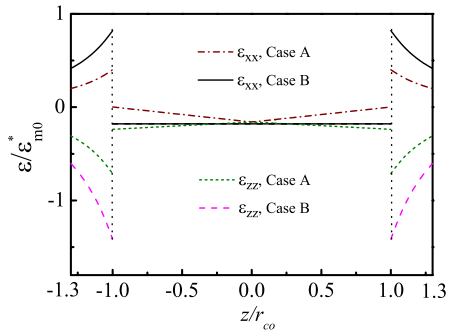

Figure 5. Distributions of normalized elastic strains $\varepsilon_{zz}/\varepsilon^*_{m0}$ and $\varepsilon_{xx}/\varepsilon^*_{m0}$ in the free-standing nano-onion $CdTe_xSe_{1-x}$ subjected to an eigenstrain $\boldsymbol{\varepsilon}^*$ in equation (9) and a surface stress τ.

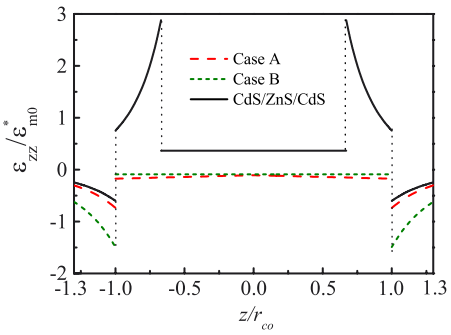

Figure 7. Distribution of normalized elastic strain $\varepsilon_{zz}/\varepsilon^*_{m0}$ in the free-standing nano-onions $Zn_xCd_{1-x}S$ and CdS/ZnS/CdS subjected to an eigenstrain $\boldsymbol{\varepsilon}^*$ in equation (9) and a surface stress τ.

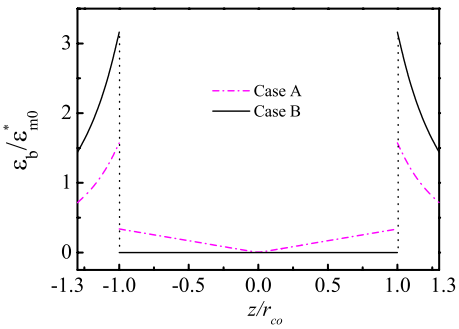

Figure 6. Distribution of normalized biaxial strain $\varepsilon_b/\varepsilon^*_{m0}$ in the free-standing nano-onion $CdTe_xSe_{1-x}$ subjected to an eigenstrain $\boldsymbol{\varepsilon}^*$ in equation (9) and a surface stress τ.

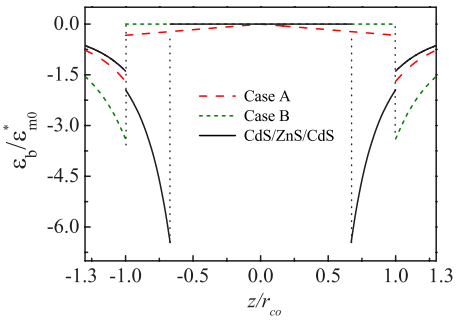

Figure 8. Distribution of normalized biaxial strain $\varepsilon_b/\varepsilon^*_{m0}$ in the free-standing nano-onions $Zn_xCd_{1-x}S$ and CdS/ZnS/CdS subjected to an eigenstrain $\boldsymbol{\varepsilon}^*$ in equation (9) and a surface stress τ.

4.2. Free-standing nano-onions with non-uniform composition

Next, we analyse the elastic strain distribution in the free-standing nano-onion $CdTe_xSe_{1-x}$(core)/CdSe(shell) (figure 2(b)) due to the misfit strain and surface stress. It is noted that the free-standing nano-onion CdTe/CdSe (figure 1(b), $M = 2$) is a special case of $CdTe_xSe_{1-x}$ (with $x(r) = 1$), and we assume that the radii of the core and shell of the $CdTe_xSe_{1-x}$ nano-onion are $r_{co} = 9$ nm and $r_{sh} = 12$ nm, respectively. The elastic constants of the core (CdTe) and shell (CdSe) bulk materials are as follows: CdTe—bulk modulus 41.9 GPa, Poisson's ratio 0.41; CdSe—bulk modulus 54.6 GPa, Poisson's ratio 0.4. The lattice constants of CdTe and CdSe are $a = 6.49$ Å and $a = 6.055$ Å, respectively. For the $CdTe_xSe_{1-x}$, we again consider two radial compositional profiles of the core (equation (13)): Case A—$b_0 = 0.8$, $b_1 = -0.4$; Case B—$b_0 = 1$, $b_1 = 0$. Case B again corresponds to a uniform core. We assume that the surface stress is $\tau = 1\ \mathrm{N\ m^{-1}}$ for the free-standing nano-onion. Figures 5 and 6 show the distributions of the normalized elastic strains $\varepsilon_{zz}/\varepsilon^*_{m0}$, $\varepsilon_{xx}/\varepsilon^*_{m0}$ and ε_b in the $CdTe_xSe_{1-x}$ nano-onion. The results show that the ratios of $\varepsilon_{zz}/\varepsilon^*_{m0}$, $\varepsilon_{xx}/\varepsilon^*_{m0}$ and ε_b are different for two cases. The elastic strains are uniform in the core for Case B, whereas they are non-uniform for Case A. However, the numerical results of the elastic strains for the two cases approach each other in the core. Contrary to those of the core, the elastic strains in the shell are vastly different, which means that they are greatly influenced by the composition of the nano-onion.

4.3. Comparison between nano-onions with uniform and non-uniform compositions

Let us compare the elastic strain distribution in the non-uniform nano-onion $Zn_xCd_{1-x}S$ with that in the nano-onion with multi-shells CdS/ZnS/CdS ($M = 3$). The elastic constants of bulk ZnS and CdS are as follows: ZnS—bulk modulus 81.6 GPa, Poisson's ratio 0.4; CdS—bulk modulus 62.3 GPa, Poisson's ratio 0.4. The lattice constants of ZnS and CdS are $a = 5.409$ Å and $a = 5.815$ Å, respectively. Therefore, the misfit strain due to the mismatch of the lattice constants of ZnS(core)/CdS(shell) is $\varepsilon^*_{m0} = -7.0\%$. We consider two cases for $Zn_xCd_{1-x}S$: Case A—$b_0 = 0.8$, $b_1 = -0.4$; Case B—$b_0 = 1$, $b_1 = 0$, and $r_{co} = 9$ nm, $r_{sh} = 12$ nm. For CdS/ZnS/CdS, $r_{co1} = 6$ nm, $r_{sh1} = 9$ nm, and $r_{sh2} = 12$ nm. Case B corresponds to a uniform core. The normalized elastic strain ($\varepsilon_{zz}/\varepsilon^*_{m0}$) and the normalized biaxial strain ($\varepsilon_b/\varepsilon^*_{m0}$) are shown in figures 7 and 8. It can be seen that the distributions of the elastic strains are strongly dependent on the compositions and structures of the nano-onions, and are different for $Zn_xCd_{1-x}S$ and CdS/ZnS/CdS ($M = 3$). Note that the elastic strain in the core ($0 \leqslant z \leqslant 1.0$) of CdS/ZnS/CdS is uniform, whereas the strain in the core of $Zn_xCd_{1-x}S$ is non-uniform.

Three factors, namely the particle size, composition, and internal structure, have been used to achieve continuous tuning of the optical properties of quantum dots [53, 60]. From figures 3–8 and the above analysis, it can be seen that the strain can be modified by adjusting the composition via

the two parameters b_0 and b_1 in the $In_xGa_{1-x}As/GaAs$ and $CdTe_xSe_{1-x}$ nano-onion systems. Likewise, the strain in nano-onions with multi-shells (figures 1(a) and (b)) can be modified by adjusting the thickness and the number (M) of the shells according to equations (1) and (3)—see figures 7 and 8. Bailey and Nie [53] have shown that continuous tuning of the optical properties of the $CdTe_xSe_{1-x}$ quantum dots can be achieved by changing the composition (Se:Te molar ratio) and the internal structure without changing the particle size. The composition changes the strain, and the strain affects the optical properties of $CdTe_xSe_{1-x}$. Moreover, Bailey and Nie [53] indicated that the tuning of the optical properties through a change in the composition and the internal structures is more advantageous than through a change in the particle size in some applications such as nanoelectronics, superlattice structures, and biological labelling.

5. Conclusions

Nano-onions can be used on their own as functional devices, besides being a constituent part of a composite medium. The mismatches of the lattice constants and thermal expansion coefficients can induce significant strains in nano-onions, which in turn will affect their physical/mechanical properties. In this paper, a theoretical study of the strains in the embedded and the free-standing nano-onions with uniform and non-uniform compositions is presented within the framework of continuum mechanics supplemented by surface elasticity. The detailed numerical results show that the strains in the nano-onions can be modified by adjusting the compositions and structures of these heterogeneous particles. The information on the strain distributions can be useful for the band structure engineering of semiconductor quantum dots.

Acknowledgments

Duan's visit to Cardiff University was funded by a Post-doctoral Fellowship from The Royal Society. Duan, Wang and Yi also acknowledge the support of the National Natural Science Foundation of China under Grant no. 10525209.

References

[1] Wiggins J, Carpenter E E and O'Connor C J 2000 *J. Appl. Phys.* **87** 5651
[2] Abe M and Suwa T 2004 *Phys. Rev.* B **70** 235103
[3] Pérez-Conde J and Bhattacharjee A K 2002 *Phys. Status Solidi* b **229** 485
[4] Borchert H, Dorfs D, McGinley C, Adam S, Möller T, Weller H and Eychmüller A 2003 *J. Phys. Chem.* B **107** 7486
[5] Abe M, Kuroda J and Matsumoto M 2002 *J. Appl. Phys.* **91** 7373
[6] Williamson A J and Zunger A 1999 *Phys. Rev.* B **59** 15819
[7] Rajeshwar K, de Tacconi N R and Chenthamarakshan C R 2001 *Chem. Mater.* **13** 2765
[8] Lauhon L J, Gudiksen M S, Wang D and Lieber C M 2002 *Nature* **420** 57
[9] Lu S Y, Wu M L and Chen H L 2003 *J. Appl. Phys.* **93** 5789
[10] Goncharenko A V 2004 *Chem. Phys. Lett.* **386** 25
[11] Lang C, Nguyen-Manh D and Cockayne D J H 2003 *J. Appl. Phys.* **94** 7067
[12] Lang C, Cockayne D J H and Nguyen-Manh D 2005 *Phys. Rev.* B **72** 155328
[13] Tersoff J 1998 *Phys. Rev. Lett.* **81** 3183
[14] Malachias A, Kycia S, Medeiros-Ribeiro G, Magalhães-Paniago R, Kamins T I and Williams R S 2003 *Phys. Rev. Lett.* **91** 176101
[15] Spencer B J and Blanariu M 2005 *Phys. Rev. Lett.* **95** 206101
[16] Patriarche G, Largeau L, Harmand J C and Gollub D 2004 *Appl. Phys. Lett.* **84** 203
[17] Lemaître A, Patriarche G and Glas F 2004 *Appl. Phys. Lett.* **85** 3717
[18] Rosenauer A, Fischer U, Gerthsen D and Förster A 1997 *Appl. Phys. Lett.* **71** 3868
[19] Selen L J M, van IJzendoorn L J and de Voigt M J A 2000 *Phys. Rev.* B **61** 8270
[20] Lelarge F, Dehaese O, Kapon E and Priester C 1999 *Appl. Phys.* A **69** 347
[21] Kret S, Benabbas T, Delamarre C, Androussi Y, Dubon A, Laval J Y and Lefebvre A 1999 *J. Appl. Phys.* **86** 1988
[22] Liao X Z, Zou J, Cockayne D J H, Leon R and Lobo C 1999 *Phys. Rev. Lett.* **82** 5148
[23] Bruls D M, Vugs J W A M, Koenraad P M, Salemink H W M, Wolter J H, Hopkinson M, Skolnick M S, Fei L and Gill S P A 2002 *Appl. Phys. Lett.* **81** 1708
[24] Rockenberger J, Tröger L, Rogach A L, Tischer M, Grundmann M, Eychmüller A and Weller H 1998 *J. Chem. Phys.* **108** 7807
[25] Gurtin M E and Murdoch A I 1975 *Arch. Ration. Mech. Anal.* **57** 291
[26] Miller R E and Shenoy V B 2000 *Nanotechnology* **11** 139
[27] Bottomley D J and Ogino T 2001 *Phys. Rev.* B **63** 165412
[28] Sharma P, Ganti S and Bhate N 2003 *Appl. Phys. Lett.* **82** 535
[29] Shenoy V B 2005 *Phys. Rev.* B **71** 094104
[30] Duan H L, Wang J, Huang Z P and Karihaloo B L 2005 *Proc. R. Soc. Lond.* A **461** 3335
[31] Duan H L, Wang J, Huang Z P and Karihaloo B L 2005 *J. Mech. Phys. Solids* **53** 1574
[32] Gao W, Yu S W and Huang G Y 2006 *Nanotechnology* **17** 1118
[33] Wang J, Duan H L, Huang Z P and Karihaloo B L 2006 *Proc. R. Soc.* A **462** 1355
[34] Yakobson B I and Smalley R E 1997 *Am. Sci.* **85** 324
[35] Itskevich I E, Lyapin S G, Troyan I A, Klipshtein P C, Eaves L, Main P C and Henini M 1998 *Phys. Rev.* B **58** R4250
[36] Little R B, El-Sayed M A, Bryant G W and Burke S 2001 *J. Chem. Phys.* **114** 1813
[37] Pérez-Conde J and Bhattacharjee A K 2003 *Phys. Rev.* B **67** 235303
[38] Faux D A and Pearson G S 2000 *Phys. Rev.* B **62** R4798
[39] Stoleru V G, Pal D and Towe E 2002 *Physica* E **15** 131
[40] Gosling T J and Willis J R 1995 *J. Appl. Phys.* **77** 5601
[41] Freund L B and Johnson H T 2001 *J. Mech. Phys. Solids* **49** 1925
[42] Quek S S and Liu G R 2003 *Nanotechnology* **14** 752
[43] He L X, Bester G and Zunger A 2004 *Phys. Rev.* B **70** 235316
[44] Sormunen J, Riikonen J, Mattila M, Sopanen M and Lipsanen H 2005 *Nanotechnology* **16** 1630
[45] Grundmann M, Stier O and Bimberg D 1995 *Phys. Rev.* B **52** 11969
[46] Chu H J and Wang J 2005 *J. Appl. Phys.* **98** 034315
[47] Cahn J W and Larche F C 1982 *Acta Metall.* **30** 51
[48] Eshelby J D 1957 *Proc. R. Soc.* A **241** 376
[49] Duan H L, Jiao Y, Yi X, Huang Z P and Wang J 2006 *J. Mech. Phys. Solids* **54** 1401
[50] Streitz F H, Cammarata R C and Sieradzki K 1994 *Phys. Rev.* B **49** 10699
[51] Müller P and Saúl K 2004 *Surf. Sci. Rep.* **54** 157
[52] Vegard L 1921 *Z. Phys.* **5** 17

[53] Bailey R E and Nie S 2003 *J. Am. Chem. Soc.* **125** 7100
[54] Zhong X H, Feng Y Y, Knoll W and Han M Y 2003 *J. Am. Chem. Soc.* **125** 13559
[55] Li Y C, Ye M F, Yang C H, Li X H and Li Y F 2005 *Adv. Funct. Mater.* **15** 433
[56] Cuenot S, Frétigny C, Demoustier-Champagne S and Nysten B 2004 *Phys. Rev.* B **69** 165410
[57] Dingreville R, Qu J M and Cherkaoui M 2005 *J. Mech. Phys. Solids* **53** 1827
[58] Gilbert B, Huang F, Zhang H, Waychunas G A and Banfield J F 2004 *Science* **305** 651
[59] Martin R M 1970 *Phys. Rev.* B **1** 4005
[60] Liang Y Q, Zhai L, Zhao X S and Xu D S 2005 *J. Phys. Chem.* B **109** 7120